



# Ionospheric responses to the 14 October 2023 annular solar eclipse over Brazil: A case study of fixed-frequency isoline variations

Igo Paulino<sup>1</sup>, Paulo Roberto Fagundes<sup>2</sup>, Ana Roberta Paulino<sup>3</sup>, Maurício José Alves Bolzam<sup>4</sup>, and Valdir Gil Pillat<sup>2</sup>

<sup>1</sup>Unidade Acadêmica de Física, Universidade Federal de Campina Grande, Campina Grande, PB, Brazil

<sup>2</sup>Instituto de Pesquisa e Desenvolvimento, Universidade do Vale do Paraíba, São José dos Campos, SP, Brazil

<sup>3</sup>Departamento de Física, Universidade Estadual da Paraíba, Campina Grande, PB, Brazil

<sup>4</sup>Departamento de Física, Universidade Federal de Jataí, Jataí, GO, Brazil

**Correspondence:** Igo Paulino (igo.paulino@df.ufcg.edu.br)

## Abstract.

This study investigates the ionospheric response to the 14 October 2023 annular solar eclipse using data from stations deployed in the Brazilian equatorial and low latitudes. While most research focuses on total electron content (TEC) and ionization reduction, this work uniquely examines the temporal evolution of fixed-frequency isolines (3–8 MHz) to evaluate variations 5 in the vertical motion and structural dynamics of the ionosphere. Observations were conducted at three stations with varying degrees of obscuration i.e., Araguatins (89%), Jataí (55%), and São José dos Campos (38%). Results demonstrate a significant reduction in the altitude of iso-frequency lines at all stations following the onset of the partial eclipse, with the most pronounced effects occurring at Araguatins due to its proximity to the eclipse path. A time lag of approximately 1.5 hours was observed between maximum obscuration and the minimum altitude of the isolines. Interestingly, a slight initial increase in altitude was 10 detected at all sites immediately after the start of the partial eclipse, likely due to plasma convergence toward the eclipse path driven by thermospheric cooling. The recovery phase was found to be latitudinally dependent as well, Araguatins (equatorial) recovered faster than the low-latitude stations, a phenomenon attributed to the interplay between the equatorial fountain effect and eclipse-induced atmospheric pressure gradients. These findings highlight that even an annular eclipse with partial obscuration 15 significantly disturbs the ionospheric dynamics over 1,500 km away from the central shadow path, emphasizing the high sensitivity of the Earth's ionosphere to transient solar occultation.

## 1 Introduction

A solar eclipse occurs when the Moon is positioned between the Earth and the Sun, momentarily blocking the sunlight. An eclipse can be observed on the Earth and classified as total, when the Moon completely obscures the Sun; annular, when the Moon does not cover the entire solar disc, creating a "ring of fire" effect; or partial, when only a portion of the Sun is blocked. 20 Total and annular eclipses can only be observed from within the umbra (the darkest part of the shadow).



These events are relatively rare and restricted to the New Moon phase. To put this in perspective, of the 228 solar eclipses that occurred in the last century, only 71 were total and 73 were annular. The complex dynamics of the Earth-Moon-Sun system result in shadow paths of varying shapes and sizes across the Earth's surface.

During a solar eclipse, the Moon's shadow typically travels at supersonic speeds ranging from 440 to 880 m/s, depending 25 on the latitude, while the umbra disc varies between 100 and 300 km in diameter. Although the physical footprint of an eclipse is relatively small, significant atmospheric effects have been observed due to the sudden blocking of sunlight.

Localized effects include cooling in the troposphere (e.g., Founda et al., 2007), heating in the stratosphere (e.g., Das et al., 2023; Paulino et al., 2025a) and enhancement in ozone concentration (e.g., Mateos et al., 2014) and relative humidity (e.g., Pratap et al., 2021). Additionally, vertical fluctuations in atmospheric fields have been recorded (e.g., Paulino et al., 2025b). 30 Furthermore, recent researches have pointed out significant differences in how the land and ocean respond to these events (e.g., Basha et al., 2025).

The combination of the pressure gradient between adjacent regions close to the eclipse path and the supersonic motion of the Moon's shadow contributes favorably to the production of atmospheric gravity waves in different layers of the atmosphere (Knizova and Mosna, 2011), traveling ionospheric disturbances (TIDs; e.g., Coster et al., 2017), and bow waves (e.g., Harding 35 et al., 2018). These waves can propagate over long distances, extending the effects of the eclipse far from the path of the umbra (e.g., Paulino et al., 2020).

Regarding the ionosphere, local effects within the path of the eclipse can be very pronounced, primarily the rate of ionization. The main source of ionospheric ionization is the absorption of the Sun's extreme ultraviolet (EUV) and X-ray radiation. The 40 blocking of sunlight during an eclipse significantly reduces the ion concentration within the ionospheric column, which is directly reflected in the F-region density and Total Electron Content (TEC) (e.g., Goncharenko et al., 2018).

The annular solar eclipse of 14 October 2023 was significant due to its trajectory over highly populated areas of the Americas. Originating in the North Pacific and concluding in the South Atlantic, the path spanned North, Central, and South Americas. Various experiments were deployed along this corridor to investigate the ionospheric response to this event (Aa et al., 2024; Ray et al., 2024; Bravo et al., 2025; Chauhan et al., 2025; He et al., 2025; Sergeeva et al., 2025).

45 In Brazil, an observation campaign was conducted that included stratospheric balloon launches (Paulino et al., 2025b), monitoring of Earth's magnetic field variations, airglow observations, ionospheric measurements, among others. The present work reports ionospheric responses recorded by the Universidade do Vale do Paraíba (UNIVAP) ionosonde network, which monitors the equatorial and low-latitude ionosphere. Data from three stations were utilized: Araguatins ( $5.64^{\circ}\text{S}$   $48.11^{\circ}\text{W}$ , dip angle  $-1.14^{\circ}$ ), Jataí ( $17.88^{\circ}\text{S}$ ,  $51.71^{\circ}\text{W}$ , dip angle  $-13.4^{\circ}$ ) and São José dos Campos ( $23.17^{\circ}\text{S}$ ,  $45.88^{\circ}\text{W}$ , dip angle  $-18.6^{\circ}$ ).

50 The first station was located very close to the eclipse path and experienced an obscuration of approximately 89%; the second and third stations reached obscurations of approximately 70% and 38%, respectively. This comparative study reveals that even during an annular event, a solar eclipse significantly disturbs the ionosphere within the umbra and its adjacent regions. In addition to previous publications, the present work focuses on the variation of fixed-frequency isolines. This approach is useful for evaluating how the vertical motion of the entire ionosphere is affected by the eclipse, a topic that remains relatively 55 unexplored, as previous research has focused more frequently on the reduction of ionospheric ionization.



## 2 Observation and instrumentation

An observational campaign was conducted in Brazil on 14 October 2023 to investigate atmospheric responses to the annular solar eclipse. Several aeronomy and space geophysics instruments were operated in coordination. Data collection included air-glow imaging, geomagnetic field variations, vertical tropospheric/stratospheric balloon soundings, and ionospheric monitoring via GNSS receivers and ionosondes.

The UNIVAP observatory network for ionospheric studies operates three Canadian Digital Ionosondes (CADIs, MacDougall et al., 1995) located at Araguatins ( $5.64^{\circ}$ S  $48.11^{\circ}$ W, dip angle  $-1.14^{\circ}$ ), Jataí ( $17.88^{\circ}$ S,  $51.71^{\circ}$ W, dip angle  $-13.4^{\circ}$ ) and São José dos Campos ( $23.17^{\circ}$ S,  $45.88^{\circ}$ W, dip angle  $-18.6^{\circ}$ ). Figure 1 shows the locations of these observational sites and includes the path of the eclipse across South America. Additionally, the path of the Moon's shadow is overplotted, with the colored line representing Universal Time.

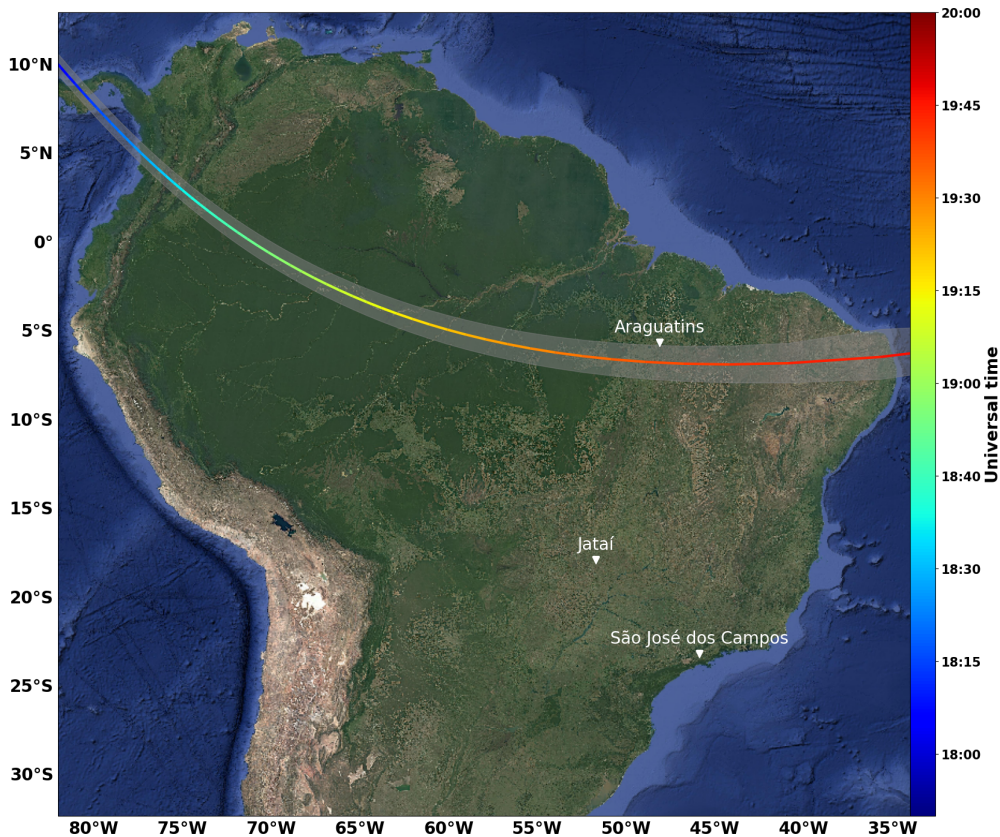


**Figure 1.** Map of South America showing the passage of the Moon's shadow on 14 October 2023 and the locations of the observatories where the CADIs are deployed. The colored line represents the Universal Time (UT) of the eclipse umbra, as referenced in the color bar. This chart was generated using the Cartopy library (Met Office, 2010 - 2015).



As illustrated, Araguatins is located very close to the umbra, whereas Jataí and São José dos Campos are further from the path of the Moon's shadow. However, all three sites were within the eclipse's penumbra and experienced partial eclipse of the Sun. Notably, these three sites are located at very similar longitudes, resulting in nearly simultaneous experiences of maximum obscuration.

70 During the campaign, the ionosondes operated in two modes: ionograms and fixed frequencies (Grant et al., 1995). Ionograms were produced with a 5-minute temporal resolution to enhance data quality during the passage of the Moon's shadow. Additionally, the ionosondes scanned six fixed frequencies (3, 4, 5, 6, 7, and 8 MHz) at a higher temporal resolution of 1.67 minutes.

75 Isolines of fixed frequencies are particularly useful for observing the temporal evolution of ionization altitude because the plasma frequency is proportional to the square root of the electron density. Consequently, these parameters provide a direct measure of the vertical motion of the entire ionosphere. Lower frequencies give information regarding the bottomside layers, whereas higher frequencies are reflected at higher altitudes. Further details regarding the operation and applications of the UNIVAP ionosondes have been published elsewhere (e.g., Fagundes et al., 2025a, b).

80 Data analysis and image processing were performed using the UNIVAP Digital Ionosonde Data Analysis (UDIDA) software (Pillat and Fagundes, 2025), which has several features for calculating ionospheric parameters from ionograms, fixed-frequency isolines, and drift modes (e.g., Pillat et al., 2013).

### 3 Results

Figure 2 shows the isolines for fixed frequencies of 3, 4, 5, 6, 7, and 8 MHz observed at Araguatins on 13, 14 and 15 October 2023 (top, middle, and bottom panels, respectively). The behavior from 00:00 to 16:00 UT across the three days is typical for this time of year. Significant scattering is observed during the nighttime, which likely indicates the presence of plasma irregularities. The temporal variation of the iso-frequencies can be interpreted as a direct response to the vertical motion of the ionosphere. Generally, all frequencies follow the diurnal variation of the ionosphere. However, the scattering observed primarily at night may reflect the presence of equatorial plasma bubbles.

90 A trend of low altitudes is visible at the start of each day, followed by a gradual increase throughout the daylight hours, this corresponds to the ionization response, particularly for the higher frequencies. Following sunset, there is a distinct enhancement in the altitudes of the plasma frequencies, which is a clear manifestation of the Pre-Reversal Enhancement (PRE). Notably, this enhancement is more pronounced at Araguatins due to its location within the equatorial region.

95 Comparing the middle panel (eclipse day) to the upper (day before) and lower (day after) panels, it is evident that following the passage of the maximum eclipse (indicated by the vertical dashed line) on 14 October 2023, there is a pronounced decrease in the altitude of all iso-frequency lines lasting approximately one hour. Following this depression, the plasma iso-frequencies recover their natural pattern of increasing altitude

The reduction in the altitude of the iso-frequencies reflects that the electron concentration is going down, which can be either decrease in ionization at the high levels or downward motion of the ionosphere. Comparing the time of the maximum eclipse



(19:37 UTC) to the minimum altitude of the iso-frequencies ( $\sim$ 21:10 UTC) at Araguatins, it is evident that the Moon's shadow 100 leads the altitude minimum by approximately 1.5 hours.

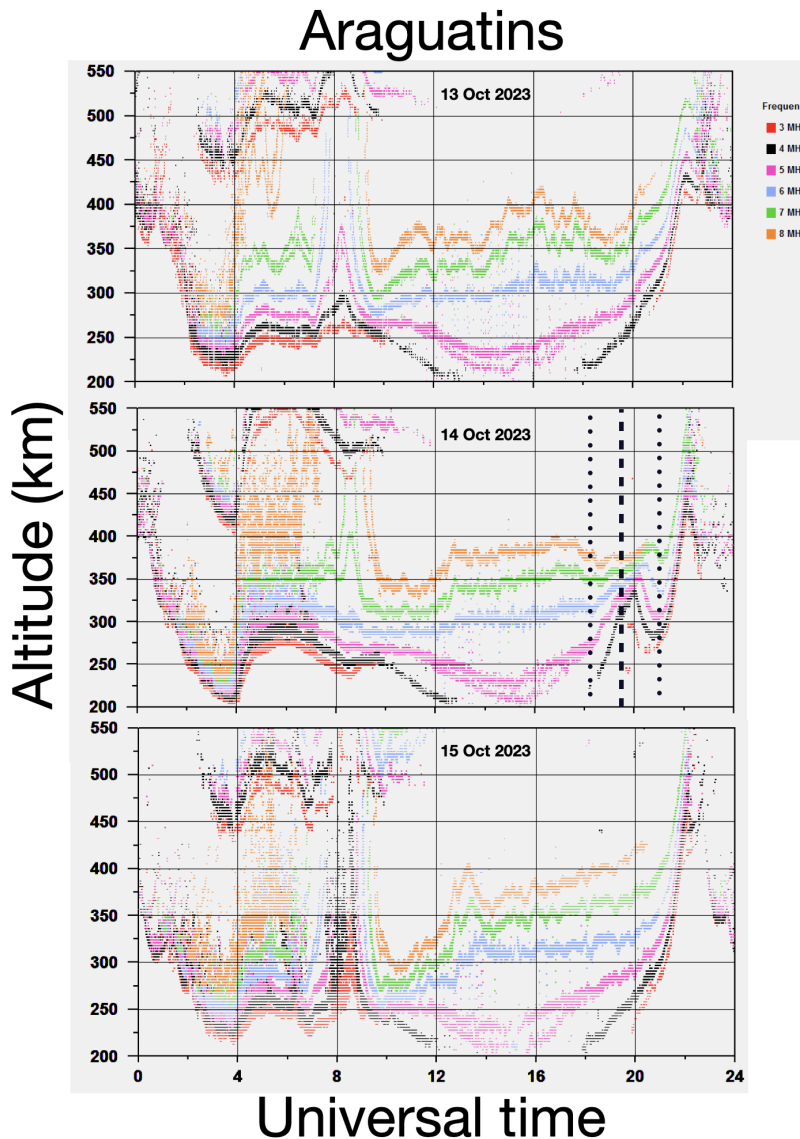


**Figure 2.** Isolines for fixed frequencies of 3, 4, 5, 6, 7, and 8 MHz (as indicated by the color legend) were measured at Araguatins. The dashed vertical line represents the time of maximum obscuration, while the vertical dotted lines indicate the start and end of the partial eclipse.

Another significant finding is the phase progression with respect to altitude, which indicates that the lower ionosphere responded rapidly to the passage of the Moon's shadow. A similar, but, less pronounced, progression is observed during the recovery phase.



Figure 3 shows the isolines for fixed frequencies measured at Jataí, comparing the days before and after the eclipse. Unfortunately, there were no measurements taken on 15 October 2023 around the time of the eclipse. However, the period preceding the eclipse passage is useful in demonstrating that the three days were quite similar, characterized by high spread during the nighttime.

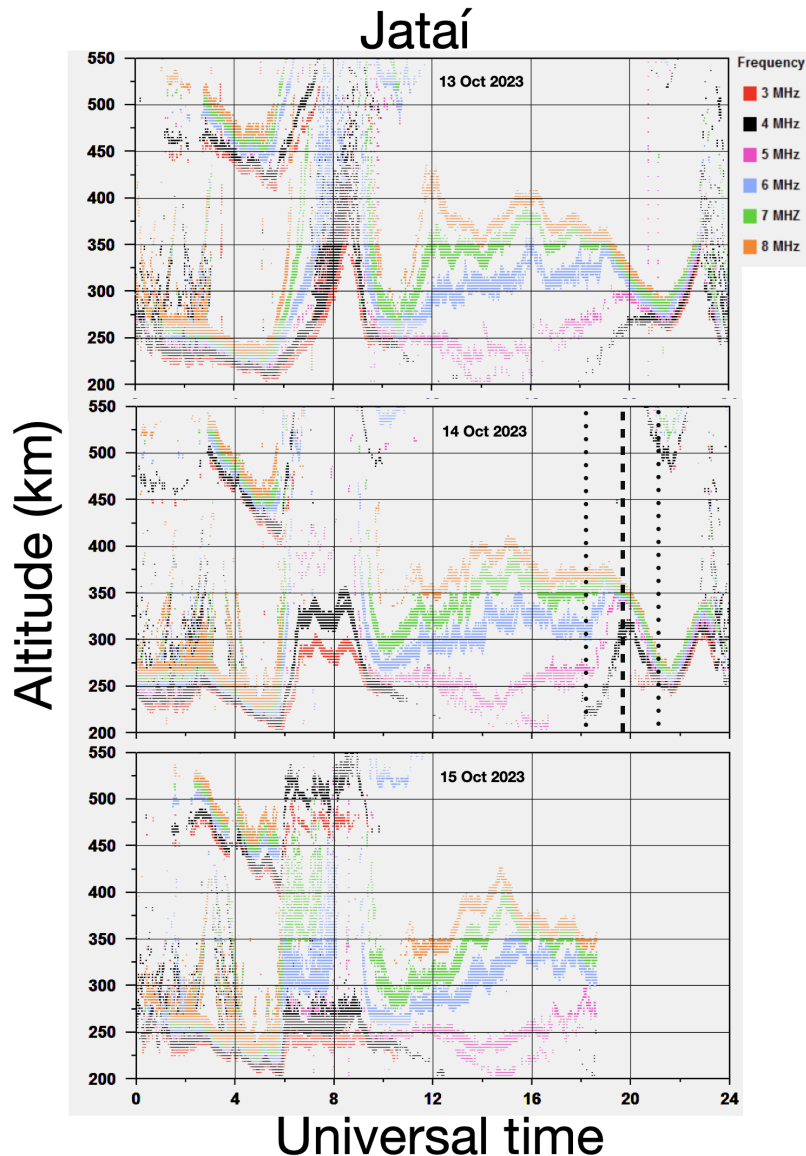


**Figure 3.** Same of Figure 2, but for Jataí.

Unlike Araguatins, the ionosphere over Jataí exhibited a weak pre-reversal enhancement effect. On both 13 and 14 October 2023, a reduction in the altitude of plasma frequencies was observed after approximately 19:00 UTC. However, on the day



110 of the eclipse, the negative slope was clearly stronger and the recovery phase was slightly delayed. Additionally, the recorded altitudes for the iso-frequencies were lower across all measured frequencies.

At Jataí, there was practically no phase difference among the isolines during either the reduction or recovery phases of the iso-frequency altitudes on the eclipse day. This represents another distinct difference in how the ionosphere responded to the eclipse at equatorial versus low latitudes.

115 Figure 4 displays the isolines for fixed frequencies at São José dos Campos. Data collected on 13 and 15 October 2025 indicate that during the period surrounding the 14 October 2023 solar eclipse, the ionosphere responded with a rapid and significant decrease in the altitude of plasma frequencies. This is a notable consequence of reduced vertical motion of the ionosphere or a reduction in the ionization in the high level caused by the occultation of sunlight.

120 The reduction of the altitude of the iso-frequencies is out of phase with the passage of the Moon's shadow, suggesting a delayed ionospheric response to the obscuration of sunlight. This delay persists into the recovery phase, even after the effects of the partial eclipse have ended.

125 A very slight progressing of the frequencies though the altitudes was observed when the iso-frequencies began to decrease. However, this was not perceptible during the recovery phase. Compared to Araguatins, this lag is minimal. Additionally, it is worth noting that the effect of the pre-reversal enhancement at São José dos Campos is significantly reduced in comparison to Araguatins.

To more efficiently evaluate the magnitude of sunlight obscuration during the eclipse at specific altitudes, the 6 MHz frequency was selected to compare the eclipse day with the preceding and following days across all three sites.

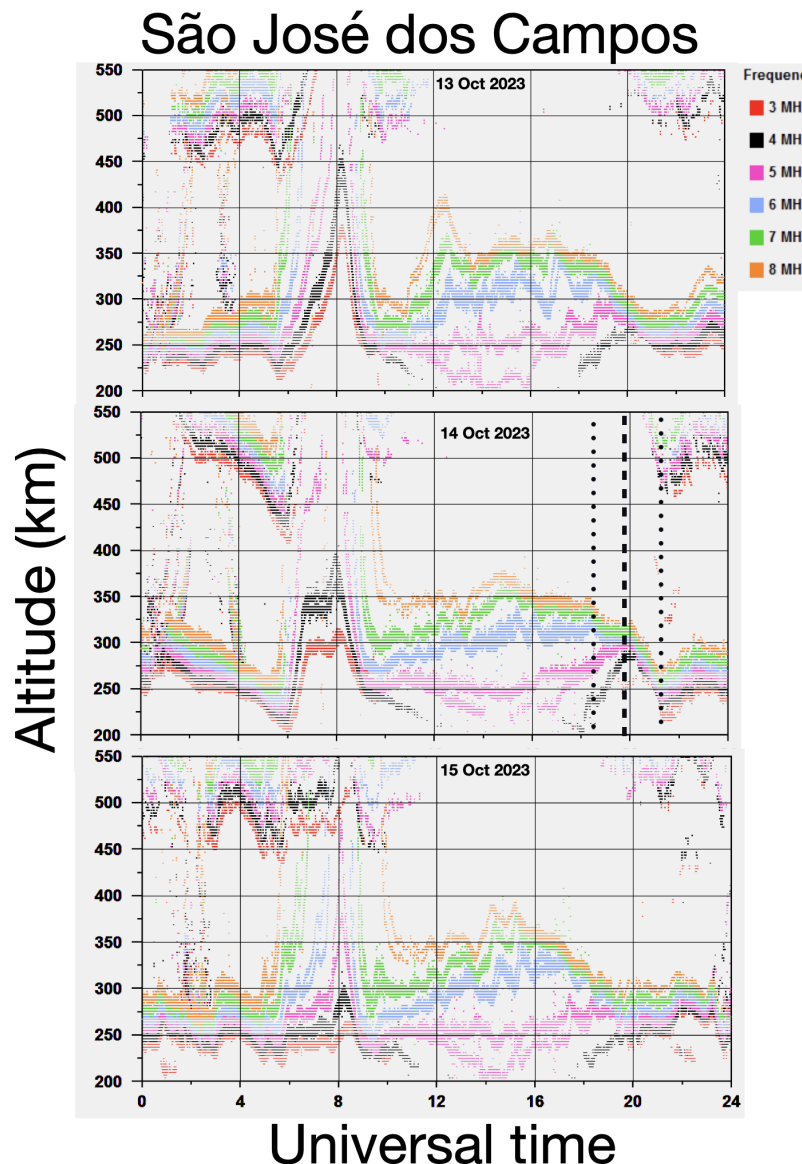


**Figure 4.** Same of Figure 2, but for São José dos Campos.

Figure 5 displays the isolines for 13 (blue curve), 14 (red curve) and 15 (green curve) October 2023, collected at Araguatins (upper panel), Jataí (middle panel), and São José dos Campos (lower panel). In these plots, vertical dash-dotted lines denote the start of the partial eclipse, solid lines mark the time of the maximum eclipse and dashed lines indicate the end of the partial eclipse. The time range was specifically chosen to encompass the period surrounding the eclipse event.

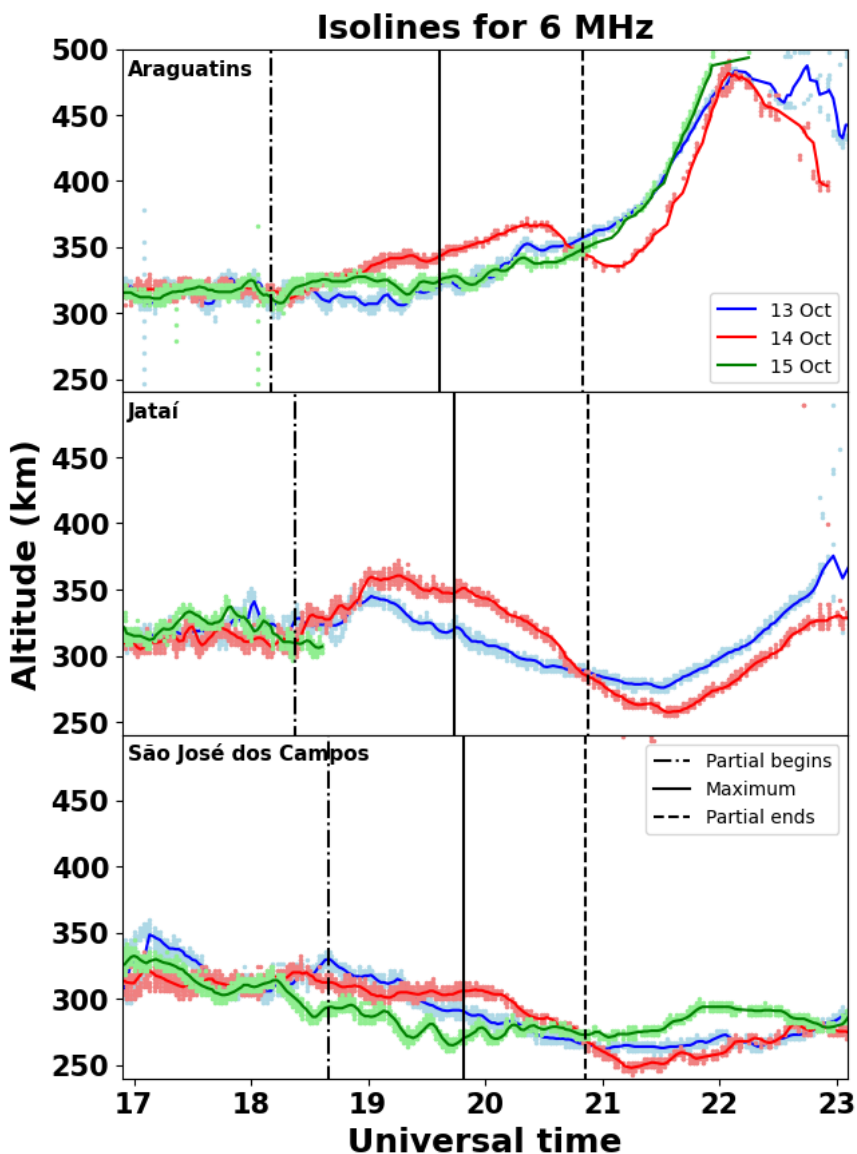


**Figure 5.** Isolines of 6 MHz frequency for three stations: Araguatins (top), Jataí (middle), and São José dos Campos (bottom). The vertical dash-dotted line represents the start of the partial eclipse, the solid line indicates the maximum obscuration and the dashed line marks the end of the partial eclipse. Observations from the day of the eclipse are shown in red, the blue and green curves represent 13 October and 15 October 2023, respectively.

Approximately one hour following the maximum eclipse at Araguatins, the 6 MHz altitude dropped by tens of kilometers. It remained suppressed relative to the control days until 22:00 UTC, underscoring a prolonged recovery phase.



135 Jataí, located at low latitudes and being the westernmost observatory, showed a plasma frequency of 6 MHz descending by several kilometers. This response occurred immediately following the maximum eclipse, though the values only fell below the 13 October 2023, baseline after the partial eclipse ended. Subsequently, the altitude remained lower until approximately 23:00 UTC. Note that data for 15 October 2023 is unavailable after 18:30 UTC.

140 The lower panel of Figure 5 displays the 6 MHz isolines for São José dos Campos across the three days. The observed behavior resembles the Jataí case, though it is less intense. Comparing the eclipse day curve to the control days (the days before and after), the altitude of the 6 MHz isoline was several kilometers lower and remained below the control curves until 22:30.

Another significant finding from these observations was a slight increase in the altitude of the 6 MHz isoline at all observation sites immediately after the start of the partial eclipse. This enhancement was more pronounced in the 4 MHz frequency curve (not shown here) and extended to the other isolines.

145 **4 Discussion and conclusions**

The absorption of sunlight is the primary mechanism for ionization in the Earth's ionosphere. A solar eclipse is physically characterized by the temporary blocking of sunlight. Thus, a reduction in ionization is expected along the eclipse path. Recent publications have quantitatively detailed this reduction within the umbra, penumbra, and partial areas. For instance, Wu et al. (2018) demonstrated a reduction of over 55% during the 21 August 2017 total solar eclipse within the umbra, while Goncharenko et al. (2018) found a 30–40% decrease as far as 1,000 km away from the eclipse's central line. Significant ionospheric responses to solar eclipses have been published in regions beyond the umbra path through the analysis of ionosonde data (e.g., Bravo et al., 2020; Resende et al., 2022).

150 An annular eclipse is a unique phenomenon for the ionospheric study because it involves a partial obscuration of sunlight that leaves a 'ring of fire'. Even when annularity reaches ~90%, the ionosphere remains illuminated by the Sun. Consequently, investigating these events, primarily through observational measurements, is essential for evaluating their impacts on the ionosphere and the atmosphere as a whole.

155 Jose et al. (2020) analyzed data collected from a meteor radar, a digisonde and a magnetometer over Trivandrum during the annular eclipse of 15 January 2010. In this comprehensive study in the Indian sector, they reported a reduction in plasma concentration of 25% in the E region (derived from  $f_oE$ ) and 29% in the F1 layer (derived from  $f_oF_1$ ). Another significant study on the effects of annular eclipses was conducted by Barad et al. (2022), who examined the 26 December 2019 solar eclipse over India and Southeast Asia. They reported a 30-40% reduction in total electron content during the passage of the Moon's shadow, the occurrence of a sporadic E layer and a decrease in temperature as recorded by the Sounding of the Atmosphere using Broadband Emission Radiometry (SABER) instrument.

160 Ray et al. (2024) used ground-based Global Navigation Satellite System (GNSS) receivers and modeling to evaluate the TEC over the Americas along the eclipse path. They found a maximum TEC reduction of approximately 50% and noted that the reduction was latitudinal-dependent, being more pronounced in middle latitudes. Results from model assimilation by He



et al. (2025) also showed this latitudinal dependency of the plasma density reduction. Similar results were reported by Aa et al. (2024), who also utilized ground-based GNSS data and model with data assimilation. Additionally, they demonstrated a vertical dependency of the TEC reduction, with the maximum depletion occurring in the F region.

170 It is important to note that the results mentioned above do not contradict the findings of this paper. In those previous cases, the percentage of TEC concentration was calculated along the eclipse path. However, in this case study, while Araguatins is located close to the path, Jataí and São José dos Campos are far from it. Consequently, these latter two sites received more solar radiation, which explains why Araguatins showed a higher sensitivity to the eclipse than the others. For instance, Chauhan et al. (2025) also demonstrated a reduction in TEC using two GNSS stations under the influence of the Moon's shadow. It was  
175 observed that the station closer to the umbra experienced a more significant reduction.

Figure 6 illustrates the temporal evolution of the eclipse percentage for the three sites. For instance, São José dos Campos reached a maximum obscuration of  $\sim 38\%$ , which is approximately half of the maximum percentage observed in Araguatins (89%). Jataí presented a maximum obscuration of  $\sim 55\%$ . Another important observation is the time lag of maximum obscuration among the three sites, which was 12 minutes. Additionally, the time lag for the beginning of the partial eclipse between  
180 Araguatins and São José dos Campos was  $\sim 30$  minutes. The end of the partial phase occurs at nearly the same time across the three locations, as it coincides with the sunset.

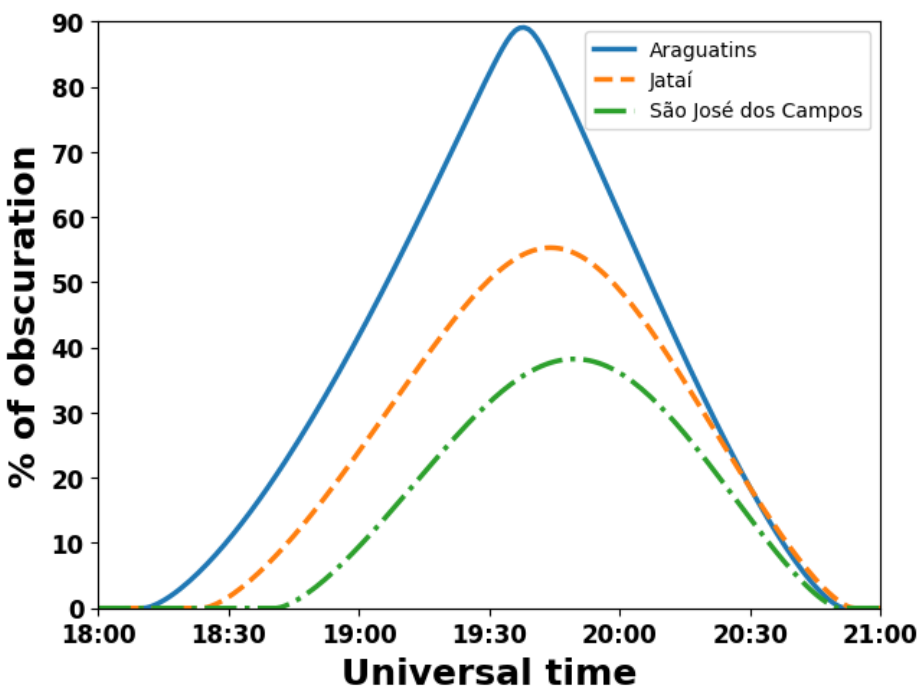


**Figure 6.** Percentagem of the solar eclipse on 14 October 2023 as a function of the time for Araguatins (solid line), Jataí (dashed line) and São José dos Campos (dash-dotted line).



Differences in ionospheric obscuration help to explain why the ionosphere over Araguatins showed a more pronounced response to the solar eclipse than the ionosphere over Jataí and São José dos Campos. Additionally, the similarities in the altitude of the fixed-frequency isolines between Jataí and São José dos Campos during the eclipse occurred because their 185 percentages of obscuration were almost the same.

Regarding the iso-frequency altitude recovery phase, the present results agree with the observations of (Aa et al., 2024). Specifically, the recovery at Araguatins was faster than at Jataí and São José dos Campos. Physically, near the equator, the ionospheric plasma is primarily controlled by fountain effects. Conversely, moving away from the equator, photochemical and diffusive processes become dominant. This is evident in the iso-frequencies presented in this work, as the altitudes at Araguatins 190 are higher and exhibit a strong signature of the pre-reversal enhancement. Additionally, the eclipse causes thermospheric cooling, which induces a gradient of pressure and results in convergence toward the eclipse region. In the equatorial region, these influences, combined with the fountain effect, can drive plasma upward, thereby mitigating the delay in the recovery phase.

The plasma convergence toward the eclipse helps explain the slight increase in iso-frequency altitudes observed prior to the 195 maximum eclipse. Ray et al. (2024) successfully simulated this behavior using the SAMI3 model and further demonstrated TEC enhancements using GNSS receiver data.

Sergeeva et al. (2025) utilized ionospheric sounding to demonstrate a reduction in  $f_oF_2$  relative to the 10-day median. Additionally, the  $h'F_2$  data indicated a slight decrease in altitude. The authors attributed the absence of more significant effects to the non-totality and short duration of the eclipse. The minimum  $f_oF_2$  value was recorded 67 minutes after maximum 200 obscuration. Notably, the characteristics of the commencement and recovery phases were remarkably similar to the results presented in this study.

The more pronounced phase progression in the descent of fixed-frequency altitudes observed at Araguatins suggests that complex equatorial electrodynamics, influenced by the equatorial electrojet, cause low iso-frequencies to descend earlier and recover more rapidly.

205 An important observation that corroborates the present results and interpretation is the vertical drift measurement calculated using the Jicamarca Unattended Long-Term studies of the Ionosphere and Atmosphere (JULIA) incoherent scatter radar at various altitudes during the 14 October 2023 solar eclipse. ? demonstrated a reduction in vertical drifts compared to control days. The downward motion of the F region, combined with the more pronounced reduction of plasma density in that layer, contributes to maintaining the iso-frequency altitudes at lower levels.

210 In summary, the present work utilized ionosonde data collected at three Brazilian sites: Araguatins, Jataí and São José dos Campos, to investigate the effects of the 14 October 2023 annular solar eclipse on the ionosphere across different levels of obscuration. While previous publications have focused on evaluating the reduction in ionization and total electron content along the eclipse path and adjacent areas, the objective of this study was to observe the temporal evolution of the altitude of fixed frequencies. This approach reveals variations in the vertical motion of the ionosphere, combined with potential differential 215 ionization across different altitudes. The main findings were:

- "A reduction in the altitude of 3–8 MHz iso-frequencies was observed at all stations after the onset of the partial eclipse



- Over Araguatins, the reduction in the altitude of iso-frequencies was more pronounced than at the other sites because of its proximity to the eclipse umbra. Consequently, the ionosphere over Jataí was more affected than over São José dos Campos;
- 220 – The recovery phase, defined as the time required for the altitudes to return to control-day values, was shortest in Araguatins, followed by Jataí and São José dos Campos. Since Araguatins is located in the equatorial region, the ionosphere is governed by the fountain effect combined with the convergence toward the eclipse path caused by thermospheric cooling. These effects act together to mitigate delays in the recovery phase;
- An increase in the altitude of the iso-frequencies was observed at all stations immediately after the commencement of 225 the partial eclipse. This could be explained by the convergence of plasma toward the eclipse path, as enhancements in Total Electron Content have been both observed and simulated with similar characteristics.

The present results confirm the high sensitivity of the ionosphere to the passage of solar eclipses. Even an annular eclipse, which preserves a "ring of fire" across its path, can significantly affect the ionosphere more than 1,500 km away from the 230 central path of the Moon's shadow, even with an obscuration of only 39%. The use of less common parameters for studying these effects, such as the altitude of iso-frequencies, highlights the profound impact of solar eclipses on both the structure and dynamics of the ionosphere.

*Data availability.* The data can be requested to Dr. Paulo Fagundes (fagundes@univap.br)

*Author contributions.* IP - Data analysis, conception and writing; PRF - Conception and revision; ARP - Calculation of the obscuration, temporal evolution of eclipse and revision; MJAB - Experiment and revision; VGP - Data analysis and revision

235 *Competing interests.* I. Paulino is member of the Annales Geophysicae Editorial Board.

*Acknowledgements.* This work has been supported by the Conselho Nacional de Desenvolvimento Científico e Tecnológico (CNPq, #309981/2023-9, #304552/2023-2, #303115/2025-4 and #403980/2025-9).



## References

Aa, E., Coster, A. J., Zhang, S.-R., Vierinen, J., Erickson, P. J., Goncharenko, L. P., and Rideout, W.: 2-D Total Electron Content and 3-D  
240 Ionospheric Electron Density Variations During the 14 October 2023 Annular Solar Eclipse, *Journal of Geophysical Research: Space  
Physics*, 129, e2024JA032447, [https://doi.org/https://doi.org/10.1029/2024JA032447](https://doi.org/10.1029/2024JA032447), 2024.

Barad, R. K., Sripathi, S., and England, S. L.: Multi-Instrument Observations of the Ionospheric Response to the 26 December 2019  
Solar Eclipse Over Indian and Southeast Asian Longitudes, *Journal of Geophysical Research: Space Physics*, 127, e2022JA030330,  
[https://doi.org/https://doi.org/10.1029/2022JA030330](https://doi.org/10.1029/2022JA030330), e2022JA030330 2022JA030330, 2022.

245 Basha, G., Ratnam, M. V., Jiang, J. H., and Pangaluru, K.: Investigating the Effects of the Solar Eclipse on the Atmosphere over Land  
and Oceanic Regions: Observations from Ground Stations and COSMIC2 Data, *Atmosphere*, 16, <https://doi.org/10.3390/atmos16070872>,  
2025.

Bravo, M., Martínez-Ledesma, M., Foppiano, A., Urrea, B., Ovalle, E., Villalobos, C., Souza, J., Carrasco, E., Muñoz, P. R., Tamblay, L.,  
Vega-Jorquera, P., Marín, J., Pacheco, R., Rojo, E., Leiva, R., and Stepanova, M.: First Report of an Eclipse From Chilean Ionosonde  
250 Observations: Comparison With Total Electron Content Estimations and the Modeled Maximum Electron Concentration and Its Height,  
*Journal of Geophysical Research: Space Physics*, 125, e2020JA027923, [https://doi.org/https://doi.org/10.1029/2020JA027923](https://doi.org/10.1029/2020JA027923), 2020.

Bravo, M. A., Fernández, J. H., Godoy, A., Pérez, J. E., Urrea, B. A., Ore, A., Carrasco, E. A., Soria, J. J., Rojo, E. D., Saavedra, C. E., Ovalle,  
E. M., Ramos, S. M., Meza, H. C., Mayhuire, G. E., Quispe, P., Vigo, E., and Poma, O.: Observations of Electric Fields during two Partial  
Solar Eclipses at the Geomagnetic Equator, *EGUsphere*, 2025, 1–19, <https://doi.org/10.5194/egusphere-2025-3155>, 2025.

255 Chauhan, V., Vishakha, Singh, R., Singh, S., Singh, V., and Singh, O. P.: The dynamic effects of solar eclipses of October 25, 2022, and October 14, 2023, on GPS-derived total electron content, *Geodesy and Geodynamics*, 16, 75–86,  
<https://doi.org/https://doi.org/10.1016/j.geog.2024.06.003>, 2025.

Coster, A. J., Goncharenko, L., Zhang, S.-R., Erickson, P. J., Rideout, W., and Vierinen, J.: GNSS Observations of  
260 Ionospheric Variations During the 21 August 2017 Solar Eclipse, *Geophysical Research Letters*, 44, 12,041–12,048,  
<https://doi.org/https://doi.org/10.1002/2017GL075774>, 2017.

Das, S. S., Kishore Kumar, K., Subrahmanyam, K. V., Venkat Ratnam, M., Suneeth, K. V., Sunilkumar, S. V., Sinha, P. R., Ghosh, A. K.,  
Das, S. K., Sonwabne, S., Muralikrishna, U. V., Kolte, Y., Naja, M., Abhilash, S., Satheesan, K., Rakesh, V., Mahesh, P., Koushik, N.,  
Satheesh Chandran, P. R., Girach, I. A., Namboodiri, K. V. S., Pandithurai, G., and Kirankumar, N. V. P.: Impact of Annular Solar Eclipse  
265 on the Trace Gases and Dynamics of the Lower and Middle Atmosphere: Results Inferred From an Integrated Campaign “Suryagrahan-2019”,  
*Earth and Space Science*, 10, e2023EA003044, <https://doi.org/https://doi.org/10.1029/2023EA003044>, 2023.

Fagundes, P., Pillat, V., Habarulema, J., Muella, M., Venkatesh, K., de Abreu, A., Anoruo, C., Vieira, F., Welyargis, K., Agyei-Yeboah,  
E., Tardelli, A., Felix, G., and Picanço, G.: Equatorial Ionization anomaly disturbances (EIA) triggered by the May 2024 solar Coronal  
Mass Ejection (CME): The strongest geomagnetic superstorm in the last two decades, *Advances in Space Research*, 76, 7375–7389,  
270 <https://doi.org/https://doi.org/10.1016/j.asr.2025.02.007>, the Powerful Solar-Terrestrial and Space Weather Event in May 2024 – Observations,  
Data and Preliminary Analysis, 2025a.

Fagundes, P. R., Pillat, V. G., Anoruo, C. M., Picanço, G. A. S., Pezzopane, M., Habarulema, J. B., Venkatesh, K., Tardelli,  
A., Christovam, A. L., and Vieira, F.: Midnight Simultaneous Observations of Spread-F and Multiple F-Layer Stratifications  
During the 11–12 May 2024 Geomagnetic Superstorm, *Journal of Geophysical Research: Space Physics*, 130, e2025JA034222,  
<https://doi.org/https://doi.org/10.1029/2025JA034222>, 2025b.



275 Founda, D., Melas, D., Lykoudis, S., Lisaridis, I., Gerasopoulos, E., Kouvarakis, G., Petrakis, M., and Zerefos, C.: The effect of the total  
solar eclipse of 29 March 2006 on meteorological variables in Greece, *Atmos. Chem. Phys.*, 7, 5543–5553, <https://doi.org/10.5194/acp-7-5543-2007>, 2007.

280 Goncharenko, L. P., Erickson, P. J., Zhang, S.-R., Galkin, I., Coster, A. J., and Jonah, O. F.: Ionospheric Response to  
the Solar Eclipse of 21 August 2017 in Millstone Hill (42N) Observations, *Geophysical Research Letters*, 45, 4601–4609,  
[https://doi.org/https://doi.org/10.1029/2018GL077334](https://doi.org/10.1029/2018GL077334), 2018.

285 Grant, I. F., MacDougall, J. W., Ruohoniemi, J. M., Bristow, W. A., Sofko, G. J., Koehler, J. A., Danskin, D., and André, D.: Comparison of  
plasma flow velocities determined by the ionosonde Doppler drift technique, SuperDARN radars, and patch motion, *Radio Science*, 30,  
1537–1549, <https://doi.org/https://doi.org/10.1029/95RS00831>, 1995.

290 Harding, B. J., Drob, D. P., Buriti, R. A., and Makela, J. J.: Nightside Detection of a Large-Scale Thermospheric Wave Generated by a Solar  
Eclipse, *Geophysical Research Letters*, 45, 3366–3373, <https://doi.org/https://doi.org/10.1002/2018GL077015>, 2018.

He, J., Yue, X., Le, H., Li, R., Li, X., Yu, Y., Liu, W., and Cao, J.: The Latitudinal Dependency of the Solar Eclipse-  
Induced Ionosphere Response on 14 October 2023, *Journal of Geophysical Research: Space Physics*, 130, e2025JA033765,  
<https://doi.org/https://doi.org/10.1029/2025JA033765>, 2025.

295 Jose, L., Vineeth, C., Pant, T. K., and Kumar, K. K.: Response of the Equatorial Ionosphere to the Annular Solar Eclipse of 15 January 2010,  
*Journal of Geophysical Research: Space Physics*, 125, e2019JA027348, <https://doi.org/https://doi.org/10.1029/2019JA027348>, 2020.

Knizova, P. K. and Mosna, Z.: Acoustic–Gravity Waves in the Ionosphere During Solar Eclipse Events, in: *Acoustic Waves - From Microde-  
vices to Helioseismology*, edited by Beghi, M. G., chap. 14, IntechOpen, London, <https://doi.org/10.5772/19722>, 2011.

MacDougall, J. W., Grant, I. F., and Shen, X.: The Canadian Advanced Digital Ionosonde: Design and Results, in: *Proceedings of the 1995  
Ionospheric Effects Symposium*, pp. 210–217, Alexandria, VA, USA, 1995.

295 Mateos, D., Antón, M., and Vaquero, J.: Influence of solar eclipse of November 3rd, 2013 on the total ozone column over Badajoz, Spain,  
*Journal of Atmospheric and Solar-Terrestrial Physics*, 112, 43–46, <https://doi.org/https://doi.org/10.1016/j.jastp.2014.02.005>, 2014.

Met Office: Cartopy: a cartographic python library with a Matplotlib interface, Exeter, Devon, <https://scitools.org.uk/cartopy>, 2010 - 2015.

300 Paulino, A. R., Paulino, I., and Pereira, J. A.: Responses of the 14 October 2023 annular solar eclipse observed in satellite temperature  
profiles, EGUsphere, 2025, 1–14, <https://doi.org/10.5194/egusphere-2025-3085>, 2025a.

305 Paulino, I., Figueiredo, C. A. O. B., Rodrigues, F. S., Buriti, R. A., Wrasse, C. M., Paulino, A. R., Barros, D., Takahashi, H., Batista,  
I. S., Medeiros, A. F., Batista, P. P., Abdu, M. A., de Paula, E. R., Denardini, C. M., Lima, L. M., Cueva, R. Y., and Makela, J. J.:  
Atmospheric Gravity Waves Observed in the Nightglow Following the 21 August 2017 Total Solar Eclipse, *Geophysical Research Letters*,  
47, e2020GL088924, <https://doi.org/https://doi.org/10.1029/2020GL088924>, 2020.

310 Paulino, I., Silva, F. R. d., Paulino, A. R., and Borba, G.: A near-sunset atmospheric sounding during the 14 October 2023 annular solar  
eclipse over Natal, EGUsphere [preprint], <https://doi.org/10.5194/egusphere-2025-6194>, received: 11 Dec 2025, 2025b.

Pillat, V. G. and Fagundes, P. R.: UDIDA Univap Digital Ionosonde Data Analysis, 2025.

Pillat, V. G., Guimarães, L. N. F., Fagundes, P. R., and da Silva, J. D. S.: A computational tool for ionosonde CADI's ionogram analysis,  
*Computers & Geosciences*, 52, 372–378, <https://doi.org/https://doi.org/10.1016/j.cageo.2012.11.009>, 2013.

Pratap, V., Kumar, A., and Singh, A. K.: Overview of solar eclipse of 21st June 2020 and its impact on solar irradiance, sur-  
face ozone and different meteorological parameters over eight cities of India, *Advances in Space Research*, 68, 4039–4049,  
<https://doi.org/https://doi.org/10.1016/j.asr.2021.08.014>, 2021.



Ray, S., Huba, J. D., Kundu, B., and Jin, S.: Influence of the October 14, 2023, Ring of Fire Annular Eclipse on the Ionosphere: A Comparison Between GNSS Observations and SAMI3 Model Prediction, *Journal of Geophysical Research: Space Physics*, 129, e2024JA032710, 2024.  
<https://doi.org/https://doi.org/10.1029/2024JA032710>, 2024.

315 Resende, L. C. A., Zhu, Y., Denardini, C. M., Chen, S. S., Chagas, R. A. J., Da Silva, L. A., Carmo, C. S., Moro, J., Barros, D., Nogueira, P. A. B., Marchezi, J. P., Picanço, G. A. S., Jauer, P., Silva, R. P., Silva, D., Carrasco, J. A., Wang, C., and Liu, Z.: A multi-instrumental and modeling analysis of the ionospheric responses to the solar eclipse on 14 December 2020 over the Brazilian region, *Annales Geophysicae*, 40, 191–203, <https://doi.org/10.5194/angeo-40-191-2022>, 2022.

320 Sergeeva, M., Gonzalez-Esparza, J., Maltseva, O., Castro-Chacon, J., Gatica-Acevedo, V., Melgarejo-Morales, A., Orrala Legorreta, I., Chiappa, X., Bonifaz, R., González-Álvarez, M., Vesnin, A., Corona-Romero, P., Rodriguez-Martinez, M., Gonzalez, L., Cabral-Cano, E., Shumaev, V., Aguilar-Rodriguez, E., Mejia-Ambriz, J., Reyes-Ruiz, M., Chernov, A., Valdes-Barron, M., Romero-Hernandez, E., Perez-Tijerina, E., Andrade-Mascote, E., and Villanueva, P.: Annular solar eclipse effects observed over Mexico on October 14, 2023: A multi-instrument study, *Advances in Space Research*, 75, 3761–3790, <https://doi.org/https://doi.org/10.1016/j.asr.2024.12.031>, 2025.

325 Wu, C., Ridley, A. J., Goncharenko, L., and Chen, G.: GITM-Data Comparisons of the Depletion and Enhancement During the 2017 Solar Eclipse, *Geophysical Research Letters*, 45, 3319–3327, <https://doi.org/https://doi.org/10.1002/2018GL077409>, 2018.